THE JOURNAL OF PHYSICAL CHEMISTRY Letters

Letter

pubs.acs.org/JPCL

CO Oxidation at the Au−Cu Interface of Bimetallic Nanoclusters Supported on CeO_2(111)

Liang Zhang, Hyun You Kim,*,† and Graeme Henkelman*

Department of Chemistry and Biochemistry, University of Texas at Austin, Austin, Texas 78712-0165, United States

Supporting Information

ABSTRACT: DFT+U calculations of the structure of CeO_2(111)-supported Au-based bimetallic nanoclusters (NCs) show that a strong support−metal interaction induces a preferential segregation of the more reactive element to the NC−CeO_2 perimeter, generating an interface with the Au component. We studied several Au-based bimetallic NCs (Au-X, X: Ag, Cu, Pd, Pt, Rh, and Ru) and found that (Au−Cu)/CeO_2 is optimal for catalyzing CO oxidation via a bifunctional mechanism. O_2 preferentially binds to the Cu-rich sites, whereas CO binds to the Au-rich sites. Engineering a two-component system in which the reactants do not compete for binding sites is the key to the high catalytic activity at the interface between the components.

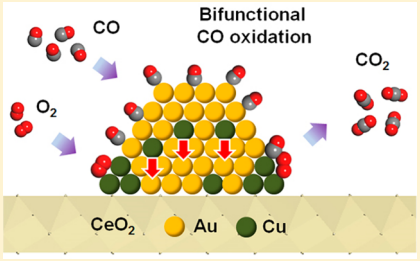

SECTION: Surfaces, Interfaces, Porous Materials, and Catalysis

The critical role of the interface between a supporting oxide and supported metal nanoparticles (NPs)/nanoclusters (NCs) has been highlighted by many experimental and theoretical studies.[1−14] Moreover, recent studies are suggesting that interfaces in nanocatalysts can be designed on the atomic scale for specific purposes. The Rodriguez and Adzic groups, in particular, have reported various kinds of tunable interfaces, metal and oxide,[9,12,15−18] metal and carbide,[19] and oxide and oxide,[2,12,17,20] and highlighted the important role of these interfaces for various heterogeneous catalytic reactions.

Since Haruta's pioneering finding on the excellent catalytic activity of oxide-supported Au NPs, the oxidation chemistry of oxide-supported Au NPs or NCs has been studied extensively, with a focus on a determination of the active site.[1,2,5,7,8] Of particular interest is how the system is able to activate the oxygen molecule to give the high catalytic activity observed experimentally. Theoretical studies of O_2 activation by supported or unsupported Au NPs/NCs have reported low O_2 binding energies and high O_2 dissociation barriers.[21] In our previous study of CO oxidation by CeO_2-supported Au NCs (Au/CeO_2), we found a relatively strong CO binding as compared with O_2 on the Au NC of Au/CeO_2(111), leading to CO poisoning and a low oxidation rate. These results suggest that a different reaction mechanism is available that involves another source of oxygen.[2] In this regard, the oxygen spillover mechanism,[1,2,6,14] the Mars−van Krevelen (M-vK) mechanism of CO oxidation,[1,14] and O_2 binding at the Au−support interface[2,4] are considered as better alternatives to explain the rich chemistry of CO oxidation by oxide-supported Au catalysts that is observed experimentally. We have previously reported that the low-coordinated interfacial oxygen atoms oxidize CO bound to Au NCs (Au-CO*) by the M-vK mechanism of CO oxidation, emphasizing the role of the NC−CeO_2 interface.[14]

We suggest a strategy to improve the catalytic activity of Au NPs/NCs by more intensive interface engineering, utilizing the strong metal−support interaction. We study a set of CeO_2(111) supported Au-based bimetallic NCs composed of 10 atoms (Au_7-X_3, where X is Ag, Cu, Pd, Pt, Rh, or Ru) and find that a strong oxygen affinity of the alloying elements, X, drives their preferential segregation to the NC-CeO_2(111) perimeter. Segregation of the metal components results in three interfaces between Au, CeO_2, and the alloying element. CO oxidation at these interfacial sites is examined using density functional theory (DFT). The different alloying elements change the reaction energetics; Cu is found to produce a particularly active CO oxidation mechanism at the interface with Au.

A 4 × 4 CeO_2(111) slab model with six atomic layers and 20 Å of vacuum was prepared to describe the CeO_2 support. Sensitivity tests on the model parameters (energy cutoff, k-point sampling, and system size) showed that our calculation parameters sufficiently describe the energetics of the oxidation catalysis by CeO_2-supported Au NP/NCs.[1,2,14] A highly symmetric hexagonal two-layered Au NC composed of 10 atoms was supported on the CeO_2(111) surface (Figure 1a). The entire Au/CeO_2 system was fully optimized prior to catalysis studies.

To study the effect of the CeO_2(111) support on the structure of supported Au-X bimetallic NPs, we replaced three Au atoms in the top layer of the Au_{10} NC with one of the following alloying elements: Ag, Cu, Pd, Pt, Rh, or Ru (Figure 1b). The preferred geometry for the alloying elements in the clusters was determined using two metrics. First, the exchange

Received: July 18, 2013
Accepted: August 10, 2013
Published: August 11, 2013

   dx.doi.org/10.1021/jz401524d | J. Phys. Chem. Lett. 2013, 4, 2943−2947

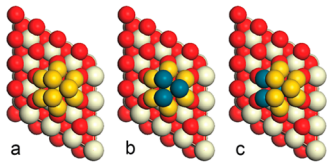

Figure 1. Au_{10} (a) and Au_7X_3 (b,c) clusters supported on the $CeO_2(111)$ surface. Yellow, ivory, and red spheres represent Au, Ce, and O atoms, respectively. Green spheres in panels b and c represent the initial and final location of alloying element. Energetics associated with the segregation of alloying element to the NC-CeO_2 interface (from b to c) are shown in Table 1.

energy E_{ex,CeO_2} is calculated as the energy gained by exchanging three alloying atoms at the top layer of the $(Au_7\text{-}X_3)/CeO_2$ with bottom-layer Au atoms, as shown in Figure 1c. A second measure is the CeO_2-induced preferential segregation energy, $E_{seg,CeO_2\text{-}Au}$, defined as the change in exchange energy between a supported cluster and a gas phase cluster, $E_{seg,CeO_2\text{-}Au} = E_{ex,CeO_2} - E_{ex,Au}$, where $E_{ex,Au}$ is the energy gained by exchanging the three alloy atoms on the surface of a gas-phase Au cluster to the subsurface. (See Figure S1 in the Supporting Information for details.) As such, $E_{seg,CeO_2\text{-}Au}$ indicates whether the bond energy between the X and the CeO_2 surface is stronger than that to Au. Calculations of CO and O_2 adsorption as well as the subsequent CO oxidation catalysis were examined on the most stable cluster.

Figure 1 shows the structure of our models: Au/CeO_2 and $(Au\text{-}X)/CeO_2$. We have previously reported that the bonding between the CeO_2 support and the supporting Au NC is governed by the hybridization of Au-5d and O-2p orbitals.[14] The same nature of bonding between the Au-X and CeO_2 support was found here. (See Figure S2 in the Supporting Information).

The calculated values of $E_{seg,CeO_2\text{-}Au}$ in the Au-X systems show that CeO_2 prefers to bond with the alloying element rather than with Au atoms, showing that the CeO_2 support induces a preferential segregation of the oxophilic element to the (Au-X)-CeO_2 perimeter. (See Table 1.) The effect of the CeO_2 support on the preferential segregation of the alloying element to the NC−CeO_2 interface is more prominent in the system where $E_{seg,CeO_2\text{-}Au}$ is greater than $E_{ex,Au}$, including Au−Cu and Au−Rh NCs. These systems, as well as the Au−Ru NC, whose $E_{seg,CeO_2\text{-}Au}$ is comparable to Au−Rh, were considered for further CO oxidation studies

In Au−Ag, Au−Pd, and Au−Pt NCs, the energy acquired from the CeO_2-X bond formation, $E_{seg,CeO_2\text{-}Au}$, is smaller than the energy gained from the surface energy reduction, $E_{ex,Au}$, indicating that the CeO_2-X bond formation is not strong enough to induce a segregation of the alloying element to the NC−CeO_2 interface. In larger NPs, therefore, the alloying element is expected to be found in the core of the Au-X NP rather than at the NP−CeO_2 interface.

A strong interaction between the CeO_2 support and supported NPs/NCs and especially on the defective or stepped CeO_2 surfaces has been previously reported.[2,14,22,23] In the case of Au NPs/NCs, a strong interaction with the support is advantageous because pinned Au NPs/NCs are less susceptible to deactivation due to thermal sintering. Adding small amounts of an oxophilic alloying element to Au NPs/NCs can generate a pinning site of Au NPs/NCs on the Au NPs/NC perimeter and increase the lifetime of the catalyst.

In a previous study of CO oxidation on the Au NC of the Au/CeO_2 by the Langmuir−Hinshelwood mechanism it was found that even though the activation energies of CO oxidation by the Au−O_2* and Au−O* are both very low, an asymmetrically strong CO binding (E_{ad} = −1.05 eV) on the Au NC hinders the coadsorption of O_2 (E_{ad} = −0.56 eV), leading to a low O_2 surface concentration and a low reaction rate.[2] In the case of this Au_{10}/CeO_2 model catalyst we confirmed again that the Au_3 top layer preferentially binds CO over O_2 so that this surface acts as a source of bound CO molecules. However, in the case of $(Au\text{-}X)/CeO_2$, we hypothesize that the oxophilic alloying element would generate a potential oxygen binding site, resulting in a different catalytic behavior as compared with the monometallic supported Au cluster. To validate our hypothesis, we calculated the binding energy of reactants (CO and O_2) on the Au−X and X−X sites of the $(Au-Cu)/CeO_2$, $(Au-Rh)/CeO_2$, and $(Au-Ru)/CeO_2$ catalysts, where the alloying element is segregated to the NC−CeO_2 interface.

Table 2 shows the energy of CO and O_2 binding on the Au-X and X-X sites of tested catalysts and corresponding surface concentration of CO and O_2 at the binding site. (The Supporting Information has details of the surface concentration calculations.) The binding sites in the Au−Ru and Au−Rh systems that bind CO more strongly than O_2 would be saturated by CO when the catalyst is exposed to the CO oxidation condition. (See Table 2.) Because these systems do not have a preferential O_2 binding site and their CO binding

Table 2. Binding Energy and Surface Concentration of CO and O_2 of Studied $(Au\text{-}X)/CeO_2$ Catalysts[a,b]

binding energy (eV)		Au−Cu	Au−Rh	Au−Ru
Au−X	O_2	−0.64	−1.02	−1.19
		(0.997)	(0.00)	(0.00)
	CO	−0.57	−1.37	−1.64
		(0.003)	(1.00)	(1.00)
X−X	O_2	−0.77	−1.57	−1.31
		(1.00)	(0.007)	(0.00)
	CO	−0.60	−1.78	−1.77
		(0.00)	(0.993)	(1.00)

[a]Binding sites are shown in Figure 2. [b]Values in the parentheses represent the surface concentration of the corresponding reactant at 298 K, $p(O_2)$ = 0.21, and $p(CO)$ = 0.01. (See the Supporting Information for details.)

Table 1. Calculated values of E_{ex,CeO_2}, $E_{ex,Au}$, and $E_{seg,CeO_2\text{-}Au}$

alloying element	Ag	Cu	Pd	Pt	Rh	Ru
E_{ex,CeO_2} (eV)	−0.89	−2.56	−1.30	−1.25	−2.63	−3.69
$E_{ex,Au}$ (eV)	−0.74	−1.17	−0.97	−0.94	−0.98	−2.08
$E_{seg,CeO_2\text{-}Au}$ (eV)	−0.15	−1.39	−0.33	−0.31	−1.65	−1.61

dx.doi.org/10.1021/jz401524d | J. Phys. Chem. Lett. 2013, 4, 2943−2947

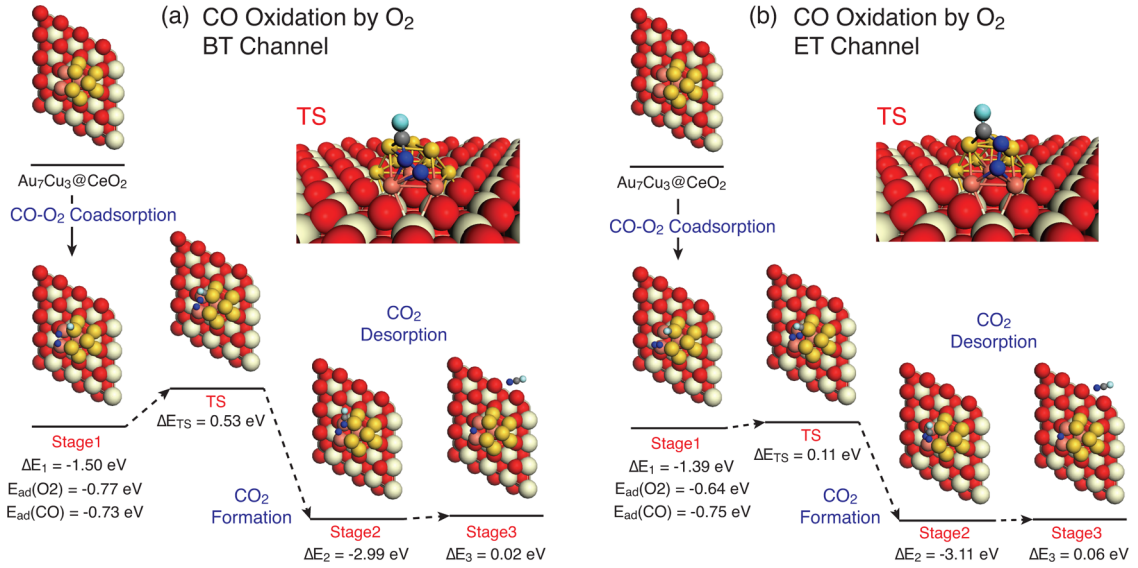

Figure 2. Two available initial CO oxidation channels catalyzed by Au_7Cu_3 NC supported on $CeO_2(111)$. The ET channel (b) provides the faster pathway with a lower activation energy (ΔE_{TS}). Ivory, red, blue, gray, and green spheres represents Ce, O (CeO_2), O (O_2), C, and O(CO) atoms, respectively. Au and Cu atoms in the Au_7Cu_3 NC were colored in yellow and copper. ΔE_x is the energy of the xth state relative to the previous stage; for example, $\Delta E2$ is the energy difference between stage 2 and stage 1.

energy is higher than that of the Au/CeO_2 system, CO poisoning at the surface of Au−Rh and Au−Ru NCs would prevent CO oxidation by the Langmuir−Hinshelwood mechanism.

We should note here that DFT at the GGA level of theory is known to have systematic errors in the binding energy of molecules, arising, for example, from the reference energy of gas-phase O_2. Thus, the relative binding energies and reaction rates between different catalysts (as reported in Table 2) should be trusted more than the absolute values.

An oxygen spillover mechanism, involving the diffusion of a lattice oxygen atom of the CeO_2 support to the supported oxophilic metal NPs/NCs, was found to be endothermic in the Au−Rh and Au−Ru systems; 0.77 and 0.63 eV in the (Au−Rh)/CeO_2 and (Au−Ru)/CeO_2, respectively. Even the O_2 binding energy in the Au−Rh and Au−Ru systems is stronger than that in Au−Cu; their absolute O_2 binding energy is far less than the vacancy formation energy of the $CeO_2(111)$ surface, which is 2.48 eV in our system. Therefore, there is no mechanism to provide a sufficient concentration of the (Au−Rh)-O* and (Au−Ru)-O* species for CO oxidation. Some caution of this result is appropriate, however, because oxygen spillover from the CeO_2 support to the supported pure Ag[24] and Pt[6] NCs/NPs has been reported. The case of Ag NPs is still controversial; Luches et al. claimed that oxygen spillover cannot occur from the $CeO_2(111)$ surface.[25] For Pt NP, oxygen spillover was reported from the low-coordinated oxygen atom of nanosized CeO_2. Modifying the oxygen binding energy to the NC by increasing the concentration of the oxophilic alloying element or decreasing the vacancy formation energy of the CeO_2 support by reducing the size may facilitate oxygen spillover and subsequent CO oxidation.

The (Au−Cu)/CeO_2 is the only system where both Au−Cu and Cu−Cu sites clearly prefer to bind O_2 more strongly than CO. The binding sites of O_2 and CO are well-separated in this system; that is, O_2 binds to the alloying atom sites, while CO binds to the Au sites.

Benefiting from its ability to separate the CO and O_2 binding sites, the (Au−Cu)/CeO_2 system was selected for analysis of its catalytic activity. Coadsorption of CO and O_2 was tested on the region of Au−Cu interface. As shown in Figure 2, the top Au sites are dominated by CO, and O_2 can binds to either bottom Cu−Cu sites or edge Au−Cu sites in a bridge geometry, initiating two possible reaction pathways. These two reaction pathways are denoted as (1) BT: where O_2 binds to the Cu−Cu sites in a bridge geometry and CO binds to the top layer Au atom and (2) ET: where O_2 binds to the Au−Cu sites in a bridge geometry and CO binds to the top layer Au atom. Figure 2 shows the overall energy profiles of two reaction pathways. The coadsorption geometry of both reaction channels is almost equally favored: ΔE_1 (BT) = −1.50 eV and ΔE_1 (ET) = −1.39 eV. Association of coadsorbed CO and O_2, which is the rate-determining step of CO oxidation by the Langmuir−Hinshelwood reaction,[2,26] produces a gas phase CO_2 and a residual Au−O* with an activation energy of 0.53 eV for the BT channel and 0.11 eV for the ET channel. The accessible O_2 adsorption geometry in the ET channel (one of the O atoms of the adsorbed O_2 molecule is close to the Au-CO* species) lowers the activation energy of the first CO oxidation step, making the ET channel the favored CO oxidation pathway.

After the first CO oxidation step, the residual Au−O* oxidized one more CO molecule, completing the CO oxidation process. Figure 3 shows the energy profile of the second CO oxidation by the Au−O*, which proceeds with an activation barrier of 0.23 eV.

We have reported atomic oxygen on the Au NCs/NPs as a highly reactive species.[2] In the case of the Au−Cu bimetallic NC, however, additional stabilizing effect from the oxophilic Cu atoms likely contributes to the increased barrier of CO oxidation by the Au−O* binding energy. We speculate that this barrier would increase as a function of the Cu concentration in the Au−Cu bimetallic NP. At higher Cu concentrations, oxygen atoms would oxidize Cu atoms, converting them to Cu_2O or CuO_2 deactivating the CO oxidation mechanism reported here.

dx.doi.org/10.1021/jz401524d | J. Phys. Chem. Lett. 2013, 4, 2943−2947

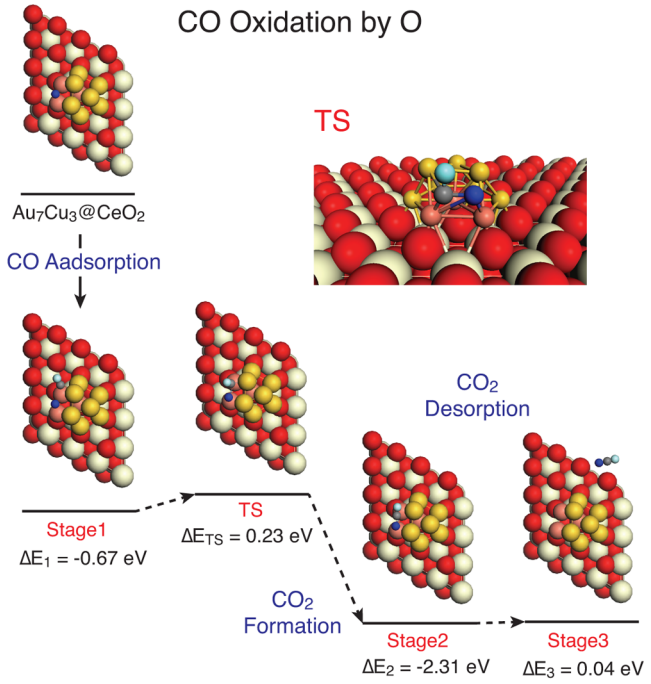

Figure 3. Reaction pathway of the CO oxidation by the residual O* atom.

The rate of CO oxidation by the (Au−Cu)/CeO_2 catalyst was estimated with a microkinetic analysis[2,26] and is presented in Table 3. (See the Supporting Information for details.)

Table 3. Microkinetic analysis of the CO oxidation mechanism involving CO and O_2 coadsorbed on the (Au−Cu) NC of the (Au−Cu)/CeO_2 catalyst

	overall activation barrier (eV)	rate (s^{-1})
Au/CeO_2[a]	0.14[a]	7.0×10^3
(Au−Cu)/CeO_2−BT[b]	0.53	1.2×10^3
(Au−Cu)/CeO_2-ET[b]	0.23	1.4×10^8

[a]Adopted from ref 2. [b]Refer to Figures 2 and 3 for the reaction pathway.

Remarkably, the rate of CO oxidation of the (Au−Cu)/CeO_2 catalyst (ET pathway) is five orders of magnitude faster than the rate of CO oxidation by the Au NC of the Au/CeO_2 system reported in our previous study.[2] Under realistic conditions, such a high reactivity is likely not possible due to mass transport limitations, but the microkinetic model clearly indicates a higher activity for the bimetallic NP. While the difference in the overall activation barriers reported in the Au/CeO_2 (0.14 eV) and (Au−Cu)/CeO_2 (0.23 eV) catalysts is small, it is the distinct binding sites for the reactions in the (Au−Cu)/CeO_2 catalyst, which leads to its high predicted activity.

COMPUTATIONAL DETAILS

We performed spin-polarized DFT calculations with the VASP code[27] using the PBE[28] functional. To treat the highly localized Ce 4f orbital, we applied DFT+U[29] with U_{eff} = 5 eV.[1,2,14] The interaction between the ionic core and the valence electrons was described by the projector-augmented wave method[30] and the valence electrons with a plane-wave basis up to an energy cutoff of 400 eV. The Brillouin zone was sampled at the Γ point. The convergence criteria for the electronic structure and the atomic geometry were 10^{-4} eV and 0.01 eV/Å, respectively. Sensitivity tests show that our results are robust with respect to the calculation and model parameters, including the k-point grid, cutoff energy, and thickness of the slab.[1,2,14] Increasing the energy cutoff to 500 eV changed the coadsorption energy of CO and O_2 on the segregated CeO_2/AuCu cluster (considering both coadsorption geometries shown in Figure 2) by <0.004 eV. A similar change in binding energy was found for increasing the k-point mesh and the slab thickness. The location and energy of transition states were calculated with the climbing-image nudged elastic band method.[31,32] Reaction energetics of CO oxidation catalysis were calculated with reference to the energy of gas-phase CO and O_2.

ASSOCIATED CONTENT

Supporting Information

Details of the microkinetic modeling as well as the exchange energy and the bonding orbitals of the supported nanoclusters. This material is available free of charge via the Internet at http://pubs.acs.org.

AUTHOR INFORMATION

Corresponding Author

*E-mail: hykim8083@gmail.com (H.Y.K.), henkelman@cm.utexas.edu (G.H.). Tel: (512) 471-4179. Fax: (512) 471-6835.

Present Address

†Hyun You Kim: Center for Functional Nanomaterials, Brookhaven National Laboratory, Upton, New York, 11973.

Notes

The authors declare no competing financial interest.

ACKNOWLEDGMENTS

This work is supported by the Department of Energy under contract DE-FG02-13ER16428. The calculations were done at the National Energy Research Scientific Computing Center and the Texas Advanced Computing Center.

REFERENCES

(1) Kim, H. Y.; Henkelman, G. CO Oxidation at the Interface between Doped CeO_2 and Supported Au Nanoclusters. *J. Phys. Chem. Lett.* **2012**, *3*, 2194−2199.

(2) Kim, H. Y.; Lee, H. M.; Henkelman, G. CO Oxidation Mechanism on CeO_2-Supported Au Nanoparticles. *J. Am. Chem. Soc.* **2012**, *134*, 1560−1570.

(3) Rodriguez, J. A.; Ma, S.; Liu, P.; Hrbek, J.; Evans, J.; Perez, M. Activity of CeO_x and TiO_x Nanoparticles Grown on Au(111) in the Water-Gas Shift Reaction. *Science* **2007**, *318*, 1757−1760.

(4) Green, I. X.; Tang, W. J.; Neurock, M.; Yates, J. T. Spectroscopic Observation of Dual Catalytic Sites During Oxidation of CO on a Au/TiO_2 Catalyst. *Science* **2011**, *333*, 736−739.

(5) Camellone, M. F.; Fabris, S. Reaction Mechanisms for the CO Oxidation on Au/CeO_2 Catalysts: Activity of Substitutional Au^{3+}/Au^+ Cations and Deactivation of Supported Au^+ Adatoms. *J. Am. Chem. Soc.* **2009**, *131*, 10473−10483.

(6) Vayssilov, G. N.; Lykhach, Y.; Migani, A.; Staudt, T.; Petrova, G. P.; Tsud, N.; Skala, T.; Bruix, A.; Illas, F.; Prince, K. C.; et al. Support Nanostructure Boosts Oxygen Transfer to Catalytically Active Platinum Nanoparticles. *Nat. Mater.* **2011**, *10*, 310−315.

(7) Carrettin, S.; Concepcion, P.; Corma, A.; Nieto, J. M. L.; Puntes, V. F. Nanocrystalline CeO_2 Increases the Activity of Au for CO Oxidation by Two Orders of Magnitude. *Angew. Chem., Int. Ed.* **2004**, *43*, 2538−2540.

(8) Guzman, J.; Carrettin, S.; Corma, A. Spectroscopic Evidence for the Supply of Reactive Oxygen during CO Oxidation Catalyzed by Gold Supported on Nanocrystalline CeO_2. *J. Am. Chem. Soc.* **2005**, *127*, 3286−3287.
(9) Bruix, A.; Rodriguez, J. A.; Ramirez, P. J.; Senanayake, S. D.; Evans, J.; Park, J. B.; Stacchiola, D.; Liu, P.; Hrbek, J.; Illas, F. A New Type of Strong Metal-Support Interaction and the Production of H_2 through the Transformation of Water on Pt/CeO_2(111) and Pt/CeO_x/TiO_2(110) Catalysts. *J. Am. Chem. Soc.* **2012**, *134*, 8968−8974.
(10) Nie, X.; Qian, H.; Ge, Q.; Xu, H.; Jin, R. CO Oxidation Catalyzed by Oxide-Supported $Au_{25}(SR)_{18}$ Nanoclusters and Identification of Perimeter Sites as Active Centers. *ACS Nano* **2012**, *6*, 6014−6022.
(11) López-Haro, M.; Cíes, J. M.; Trasobares, S.; Pérez-Omil, J. A.; Delgado, J. J.; Bernal, S.; Bayle-Guillemaud, P.; Stéphan, O.; Yoshida, K.; Boyes, E. D.; et al. Imaging Nanostructural Modifications Induced by Electronic Metal−Support Interaction Effects at Au||Cerium-Based Oxide Nanointerfaces. *ACS Nano* **2012**, *6*, 6812−6820.
(12) Park, J. B.; Graciani, J.; Evans, J.; Stacchiola, D.; Senanayake, S. D.; Barrio, L.; Liu, P.; Sanz, J. F.; Hrbek, J.; Rodriguez, J. A. Gold, Copper, and Platinum Nanoparticles Dispersed on CeO_x/TiO_2(110) Surfaces: High Water-Gas Shift Activity and the Nature of the Mixed-Metal Oxide at the Nanometer Level. *J. Am. Chem. Soc.* **2010**, *132*, 356−363.
(13) Stamatakis, M.; Christiansen, M. A.; Vlachos, D. G.; Mpourmpakis, G. Multiscale Modeling Reveals Poisoning Mechanisms of MgO-Supported Au Clusters in CO Oxidation. *Nano Lett.* **2012**, *12*, 3621−3626.
(14) Kim, H. Y.; Henkelman, G. CO Oxidation at the Interface of Au Nanoclusters and the Stepped-CeO_2(111) Surface by the Mars-van Krevelen Mechanism. *J. Phys. Chem. Lett.* **2013**, *4*, 216−221.
(15) Kowal, A.; Li, M.; Shao, M.; Sasaki, K.; Vukmirovic, M. B.; Zhang, J.; Marinkovic, N. S.; Liu, P.; Frenkel, A. I.; Adzic, R. R. Ternary Pt/Rh/SnO_2 Electrocatalysts for Oxidizing Ethanol to CO_2. *Nat. Mater.* **2009**, *8*, 325−330.
(16) Zhou, W.-P.; An, W.; Su, D.; Palomino, R.; Liu, P.; White, M. G.; Adzic, R. R. Electrooxidation of Methanol at SnO_x−Pt Interface: A Tunable Activity of Tin Oxide Nanoparticles. *J. Phys. Chem. Lett.* **2012**, *3*, 3286−3290.
(17) Park, J. B.; Graciani, J.; Evans, J.; Stacchiola, D.; Ma, S. G.; Liu, P.; Nambu, A.; Sanz, J. F.; Hrbek, J.; Rodriguez, J. A. High Catalytic Activity of Au/CeO_x/TiO_2(110) Controlled by the Nature of the Mixed-Metal Oxide at the Nanometer Level. *Proc. Natl. Acad. Sci. U. S. A.* **2009**, *106*, 4975−4980.
(18) Senanayake, S. D.; Stacchiola, D.; Rodriguez, J. A. Unique Properties of Ceria Nanoparticles Supported on Metals: Novel Inverse Ceria/Copper Catalysts for CO Oxidation and the Water-Gas Shift Reaction. *Acc. Chem. Res.* **2013**, DOI: 10.1021/ar300231p.
(19) Vidal, A. B.; Feria, L.; Evans, J.; Takahashi, Y.; Liu, P.; Nakamura, K.; Illas, F.; Rodriguez, J. A. CO_2 Activation and Methanol Synthesis on Novel Au/TiC and Cu/TiC Catalysts. *J. Phys. Chem. Lett.* **2012**, *3*, 2275−2280.
(20) Stacchiola, D. J.; Senanayake, S. D.; Liu, P.; Rodriguez, J. A. Fundamental Studies of Well-Defined Surfaces of Mixed-Metal Oxides: Special Properties of MO_x/TiO_2(110) {M = V, Ru, Ce, or W}. *Chem. Rev.* **2013**, *113*, 4373−4390.
(21) Roldan, A.; Ricart, J. M.; Illas, F.; Pacchioni, G. O_2 Adsorption and Dissociation on Neutral, Positively and Negatively Charged Au_n (n=5−79) Clusters. *Phys. Chem. Chem. Phys.* **2010**, *12*, 10723−10729.
(22) Ta, N.; Liu, J.; Chenna, S.; Crozier, P. A.; Li, Y.; Chen, A.; Shen, W. Stabilized Gold Nanoparticles on Ceria Nanorods by Strong Interfacial Anchoring. *J. Am. Chem. Soc.* **2012**, *134*, 20585−20588.
(23) Farmer, J. A.; Campbell, C. T. Ceria Maintains Smaller Metal Catalyst Particles by Strong Metal-Support Bonding. *Science* **2010**, *329*, 933−936.
(24) Kong, D.; Wang, G.; Pan, Y.; Hu, S.; Hou, J.; Pan, H.; Campbell, C. T.; Zhu, J. Growth, Structure, and Stability of Ag on CeO_2(111): Synchrotron Radiation Photoemission Studies. *J. Phys. Chem. C* **2011**, *115*, 6715−6725.
(25) Luches, P.; Pagliuca, F.; Valeri, S.; Illas, F.; Preda, G.; Pacchioni, G. Nature of Ag Islands and Nanoparticles on the CeO_2(111) Surface. *J. Phys. Chem. C* **2011**, *116*, 1122−1132.
(26) Falsig, H.; Hvolbaek, B.; Kristensen, I. S.; Jiang, T.; Bligaard, T.; Christensen, C. H.; Nørskov, J. K. Trends in the Catalytic CO Oxidation Activity of Nanoparticles. *Angew. Chem., Int. Ed.* **2008**, *47*, 4835−4839.
(27) Kresse, G.; Furthmuller, J. Efficient Iterative Schemes for Ab Initio Total-Energy Calculations Using a Plane-Wave Basis Set. *Phys. Rev. B* **1996**, *54*, 11169−11186.
(28) Perdew, J. P.; Burke, K.; Ernzerhof, M. Generalized Gradient Approximation Made Simple. *Phys. Rev. Lett.* **1996**, *77*, 3865−3868.
(29) Dudarev, S. L.; Botton, G. A.; Savrasov, S. Y.; Humphreys, C. J.; Sutton, A. P. Electron-Energy-Loss Spectra and the Structural Stability of Nickel Oxide: An LSDA+U Study. *Phys. Rev. B* **1998**, *57*, 1505−1509.
(30) Blochl, P. E. Projector Augmented-Wave Method. *Phys. Rev. B* **1994**, *50*, 17953.
(31) Henkelman, G.; Jonsson, H. Improved Tangent Estimate in the Nudged Elastic Band Method for Finding Minimum Energy Paths and Saddle Points. *J. Chem. Phys.* **2000**, *113*, 9978−9985.
(32) Henkelman, G.; Uberuaga, B. P.; Jonsson, H. A Climbing Image Nudged Elastic Band Method for Finding Saddle Points and Minimum Energy Paths. *J. Chem. Phys.* **2000**, *113*, 9901−9904.